International Journal of Biological Macromolecules 242 (2023) 124794

Contents lists available at ScienceDirect

International Journal of Biological Macromolecules

journal homepage: www.elsevier.com/locate/ijbiomac

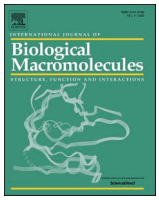

Exploring the stabilizing effect on the i-motif of neighboring structural motifs and drugs

Judit Rodriguez [a], Arnau Domínguez [b], Anna Aviñó [b], Gigliola Borgonovo [c], Ramon Eritja [b], Stefania Mazzini [c], Raimundo Gargallo [a,*]

[a] Department of Chemical Engineering and Analytical Chemistry, Faculty of Chemistry, University of Barcelona, Marti i Franqués 1-11, E-08028 Barcelona, Spain
[b] Institute for Advanced Chemistry of Catalonia (IQAC), CSIC, Networking Center on Bioengineering, Biomaterials and Nanomedicine (CIBER-BBN), Barcelona, Spain
[c] Department of Food, Environmental and Nutritional Sciences (DEFENS), University of Milan (Università degli Studi di Milano), Milan, Italy

ARTICLE INFO

Keywords:
I-motif
Duplex
Tetrad
Ligands
Stability
Multivariate analysis

ABSTRACT

Cytosine-rich DNA sequences may fold into a structure known as i-motif, with potential in vivo modulation of gene expression. The stability of the i-motif is residual at neutral pH values. To increase it, the addition of neighboring moieties, such as Watson-Crick stabilized loops, tetrads, or non-canonical base pairs have been proposed.

Taking a recently described i-motif structure as a model, the relative effect of these structural moieties, as well as several DNA ligands, on the stabilization of the i-motif has been studied. To this end, not only the original sequence but different mutants were considered. Spectroscopic techniques, PAGE, and multivariate data analysis methods have been used to model the folding/unfolding equilibria induced by changes of pH, temperature, and the presence of ligands.

The results have shown that the duplex is the moiety that is responsible of the stabilization of the i-motif structure at neutral pH. The T:T base pair, on the contrary, shows little stabilization of the i-motif. From several selected DNA-binding ligands, the G-quadruplex ligand BA41 is shown to interact with the duplex moiety, whereas non-specific interaction and little stabilization has been observed within the i-motif.

1. Introduction

DNA sequences may form characteristic structures apart from the well-known B-DNA double helix. Among these, the i-motif structure is observed in cytosine-rich DNA sequences. The i-motif is formed by the interaction of four cytosine stretches forming two parallel duplexes running in an antiparallel way. These stretches may be part of just one or more DNA strands. The building block of the i-motif is the $C{\cdot}C^{+}$ base pair, which is stabilized by the formation of three hydrogen bonds. This base pair, however, involves the protonation of a cytosine base. Because the cytosine has a pK_a around 4.5 (at 25 °C and 0.1 M ionic strength), the i-motif structures is particularly stable at pH values around this pK_a, and up to 6.5, approximately [1,2]. Important factors, such as the length of cytosine tracts and nature of the loops strongly influence on the stability of this structure [3,4].

In the human extracellular environment (pH 7.4, 37 °C and relatively high ionic strength), the i-motif is not stable, and it would eventually unfold. Because of this, the i-motif structures were largely considered only existing in vitro. Recently, however, the presence of i-motif structures was observed in cell lines [5,6]. This discovery opened the door for the search of molecules, such as proteins, ligands or acidic microenvironments that could promote the formation of these structures. It has been suggested that several ligands may interact with i-motif structures [7]. However, other studies pointed to the existence of non-specific interactions in the case of these structures [8,9]. Moreover, research is being done to determine the role of some DNA moieties, such as duplex, junctions and others, on i-motif structure. These hybrid structures are of special interest as they seem to coexist several structural domains at neutral conditions [10,11]. Apart from the biological aspects of this structure, the sharp pH-induced conformational change of the i-motif has been shown to be a potential tool in Nanotechnology [12], and as a potential pH sensor in chemical analysis [13].

In a recent work, Serrano-Chacón et al. determined the three-dimensional structure adopted by the IDJ1 cytosine-rich sequence [14]. This adopts a characteristic hybrid i-motif/duplex (or junction) structure (PDB ID 7O5E), which is very stable in front of temperature

* Corresponding author.
E-mail address: raimon_gargallo@ub.edu (R. Gargallo).

https://doi.org/10.1016/j.ijbiomac.2023.124794
Received 13 March 2023; Received in revised form 18 April 2023; Accepted 25 April 2023
Available online 12 May 2023

changes at neutral pH (Fig. 1). From the study of several IDJ1 mutants by NMR and melting experiments, the authors observed that the presence of the duplex moiety increased dramatically the thermal stability of the i-motif at neutral pH. Also, the presence of a G:T:G:T tetrad, and of a T:T base pair contributed to increase the thermal stability of the i-motif [15].

In the present work, we study the influence of these structural motifs on the stability of the overall structure in front of temperature and pH changes from a thermodynamic perspective, which complement the results obtained in the previous structural study. To this end, acid-base and melting experiments were done, and the spectra measured along the experiments were analyzed by means of multivariate data analysis methods. In addition, the potential stabilizing effect of several ligands on the resulting structure adopted by IDJ1 was studied (Fig. 1). These include five molecules that have been shown to interact with G-quadruplex (curaxin, MK4827, ABT 888, LOM1392, and BA41) ([16] and references therein), as well as four polyphenols (synaptic acid, quercetin, (+)-catechin and resveratrol), the palmatine alkaloid [17], and the TMPyP4 porphyrin [18,19].

The results have shown that the duplex moiety is the most important contribution to the thermal stability of i-motif structures at pH 7.4 and 25 °C. The second most important contribution is the G:T:G:T tetrad, and residual stabilization is provided by the T:T base pair. Spectroscopically monitored acid-base titrations and multivariate analysis allowed a detailed description of the pH-induced conformational equilibria in these sequences. It was observed that the addition of the duplex moiety greatly shifts the $pH_{1/2}$ of i-motif structure, providing additional stability at neutral pH. Thermodynamic, as well as structural information provided by NMR, indicated that the studied ligands mainly interact with the duplex moiety of the structure adopted by IDJ1, without any dramatic stabilization of the i-motif.

2. Experimental section

2.1. Reagents

The DNA sequences (Table 1) were synthesized on an Applied Biosystems 3400 DNA synthesizer using the 1 μmol scale synthesis cycle. Standard phosphoramidites were used. Ammonia deprotection was performed overnight at 55 °C. The resulting products were purified using Glen-Pak Purification Cartridge (Glen Research, USA). DNA strand concentration was determined by absorbance measurements (260 nm) at 90 °C using the extinction coefficients calculated using the nearest-neighbor method as implemented on the OligoCalc webpage [20]. Before any experiment, DNA solutions were first heated at 95 °C for 20 min and then allowed to reach room temperature overnight. The compounds BA41 and LOM1392 were prepared as reported in the literature [21,22]. Curaxin (CBL 0137) was purchased from Carbosynth Limited, Compton, UK. Compound ABT888 was purchased from ChemScene LLC, Monmouth Junction, NJ, USA. Compound MK4827 was purchased from Key Organics, Cornwall, UK. The corresponding hydrochlorides were prepared by treatment with 4 M of HCl in dioxane. Polyphenols (synaptic acid, quercetin, (+)-catechin and resveratrol), were kindly provided by Dr. Óscar Núñez (University of Barcelona, Spain) and purchased from Sigma-Aldrich (USA). The palmatine alkaloid was obtained from plant material in the Department of Biochemistry, Masaryk University (Brno, Czech Rep.). The mesotetrakis-(*N*-methyl-4-pyridyl)-porphyrin (TMPyP4) was purchased from Porphyrin Systems (Germany). KH_2PO_4, K_2HPO_4, HCl and LiOH were purchased from Panreac (Spain). MILLIQ water was used in all experiments.

2.2. Instruments and procedures

Absorbance spectra were recorded on an Agilent 8453 diode array spectrophotometer. The temperature was controlled by means of an 89090A Agilent Peltier device. Hellma quartz cells (1- or 10-mm path length, and 350, 1500 or 3000 μL volume) were used. Circular dichroism (CD) spectra were recorded on a Jasco J-815 spectropolarimeter equipped with a temperature control unit. Hellma quartz cells (10 mm path length, 1400 and 3000 μL volume) were used. Molar ellipticity ($deg \cdot cm^2 \cdot mol^{-1}$) has been calculated according to: $[\Theta] = \Theta/C \cdot l$, where Θ is the measured ellipticity (mdeg), C is the analytical concentration ($mol \cdot L^{-1}$), and l is the optical path (cm).

Spectroscopically monitored acid-base titrations were monitored by CD and/or molecular absorption spectroscopies. In all cases, experimental conditions were 20 °C and 20 mM phosphate buffer. Titrations were carried out by adjusting the pH of 1.5 mL solutions containing the oligonucleotides at 2 μM by addition of concentrated LiOH or HCl solutions. pH was measured using an Orion SA 720 pH/ISE meter and a micro-combination pH electrode (Thermo Scientific, USA). Absorbance

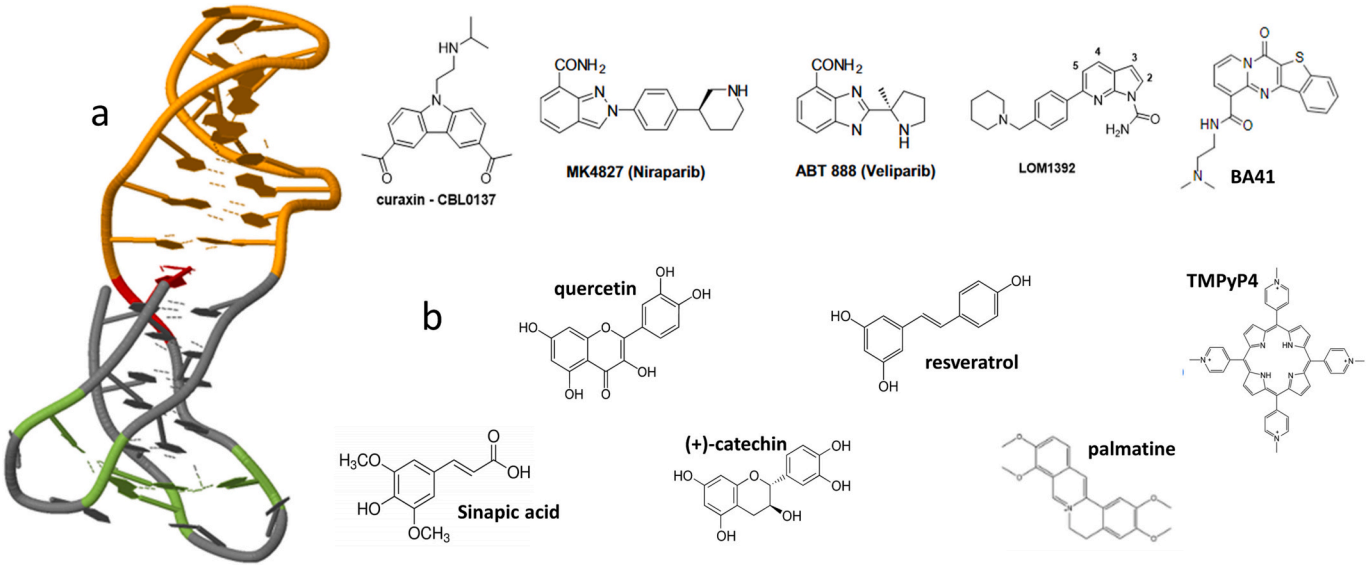

Fig. 1. (a) Structure adopted by IDJ1 sequence, according to Serrano-Chacón et al. (PDB number 7O5E). The nucleotides have been colored according to the sequence shown in Table 1: i-motif (grey), duplex (orange), G:T:G:T tetrad (green), and T:T base pair (red). (b) Molecules studied in this work as potential ligands of IDJ1.

Table 1
DNA sequences studied in this work. Bases participating in duplex, G:T:G:T tetrad, and T:T base pairs are highlighted in orange, green, and red, respectively. C bases involved in the i-motif core are underlined.

DNA	Sequence (5′ → 3′)	Length	Epsilon
IDJ1	CCC GTTT CC TCG CGA AGC ATT CGC G CCC GTTT CC T	35	319,400
IDJ1noduplex	CCC GTTT CC TC-TTT-CCC GTTT CC T	24	190,800
IDJ1notetrad	CCC TT CC TCG CGA AGC ATT CGC G CCC TT CC T	31	259,400
IDJ1noTs	CCC GTT CC CG CGA AGC ATT CGC G CCC GTT CC	31	266,100
duplexIDJ1	CGC GAA GCA TTC GCG	15	140,200

or CD spectra were recorded simultaneously in a pH stepwise fashion by using the J-815 spectropolarimeter. Hellma quartz cells (10 mm path length, 3 mL volume) were used.

Melting experiments were monitored either using the Agilent-8453 spectrophotometer or the Jasco J-815 spectropolarimeter, both equipped with Peltier units for temperature control. The DNA solution was transferred to a covered 10-mm-path-length cell and spectra were recorded at 2 °C intervals with a hold time of 3 min at each temperature, which yielded an average heating rate of approximately 0.6 °C·min^{-1}. Buffer solutions were 20 mM phosphate or acetate.

Polyacrylamide gel electrophoresis assays were performed in an 8 % nondenaturing acrylamide/bisacrylamide 29:1 gel containing 50 mM HEPES (pH 7.2), supplemented with 5 % glycerol. Samples were prepared by adding the oligonucleotide and in some cases the ligand in a 1:3 ratio in 20 mM phosphate buffer, pH 7.4. The final concentration of oligonucleotide in the sample was 34 μM. Before loading, the samples were incubated at 37 °C for 30 min. Then, the gel was run for 6 h at a fixed voltage of 140 V (10 °C) using a running buffer containing 50 mM HEPES (pH 7.2) and 20 mM $MgCl_2$. Finally, the gel was stained using a solution of 0.01 % stains-all in formamide/H_2O 1:1.

Molecular fluorescence spectra were measured with a JASCO FP-6200 spectrofluorimeter. The fluorescence spectra were monitored by using a quartz cuvette with a 10-mm path length, with the excitation and emission slits set at 10 nm, the scan speed at 250 nm/min and the temperature set at 10 °C. The measurements were taken at 365 nm excitation wavelength and emission was recorded from 430 to 700 nm. The buffer consisted of 20 mM phosphate buffer, pH 7.4. The concentration of the ligand was 3 μM, whereas the concentration of the considered DNA sequence was increased. Additionally, the titration of DNA sequences was carried out at 2.4 μM with a ligand stock solution prepared in the same buffer conditions.

The NMR samples were prepared at a concentration of 1.6 mM in 0.6 mL (H_2O/D_2O 9:1) buffer solution 20 mM potassium phosphate buffer at pH 7.4. Oligonucleotide solution was heated to 95 °C for 20 min and then allowed to reach room temperature overnight. NMR spectra were recorded on 600 MHz Bruker Avance spectrometer. Monodimensional proton spectra were recorded using pulsed-field gradient for H_2O suppression. Stock solution of the BA41 was prepared in DMSO-d_6. ^{1}H NMR titration was performed at 5 °C by adding increasing amounts of ligand to the DNA at different ratios: R = [drug]/[DNA].

2.3. Data analysis

2.3.1. Melting experiments

For melting experiments, absorbance, or CD data as a function of temperature at one single wavelength (univariate data) were analyzed as described elsewhere [23]. The physico-chemical model is related to the thermodynamics of DNA unfolding. Hence, for the unfolding of intramolecular structures such as those studied here, the chemical equation and the corresponding equilibrium constant may be written as:

$$\text{DNA folded} + \text{heat} \leftrightarrow \text{DNA unfolded}\ K_{\text{unfolding}} = [\text{DNA unfolded}]/[\text{DNA folded}] \quad (1)$$

For melting experiments, the concentration of the folded and unfolded forms is temperature dependent. Accordingly, the equilibrium constant depends on temperature according to the van't Hoff equation [24]:

$$ln\ K_{\text{unfolding}} = -\Delta H/RT + \Delta S/R \quad (2)$$

It is assumed that ΔH and ΔS will not change throughout the range of temperatures studied here. Also, it is assumed that the transition is a two-state process, without intermediates. This assumption may be checked by means of multivariate analysis methods [25].

Additionally, the complete set of CD or absorbance spectra recorded along a melting experiment were analyzed by means of a previously described multivariate method [26]. Briefly, the spectra were arranged in a table or data matrix **D**, with *m* rows (spectra recorded) and *n* columns (wavelengths at which ellipticity or absorption were measured). Then, data matrix **D** was decomposed according to Beer-Lambert-Bouer's law in matrix form:

$$\mathbf{D} = \mathbf{C}\,\mathbf{S}^{\mathbf{T}} + \mathbf{E} \quad (3)$$

where **C** is the matrix containing the concentration profiles of the considered species, $\mathbf{S}^{\mathbf{T}}$ is the matrix containing the spectra corresponding to each one of these species, and **E** is the matrix of data not explained by the proposed model. According to the decomposition of experimental data according to Eq. (3), for melting experiments monitored with molecular absorption spectroscopy the units in **C** are given as concentration (mol·L^{-1}), whereas the units in **S** are the corresponding molar absorptivity values (L·mol^{-1}). Accordingly, for melting experiments monitored with CD spectroscopy, where the experimental data are given as millidegrees (mdeg), the units in **C** are the concentration (mol·L^{-1}), whereas the units in **S** are molar ellipticities (L·mol^{-1}·mdeg^{-1}). The goodness of the model is usually evaluated by the lack-of-fit.

2.3.2. Acid-base titrations

As in the case of melting experiments, data from acid-base titrations were analyzed by means of univariate and multivariate methods. Here, CD and molecular absorption spectra recorded along acid-base titrations were monitored in a range of wavelengths from 220 to 320 nm. Later, they were arranged in a table or data matrix **D**, with *m* rows (spectra recorded) and *n* columns (wavelengths at which ellipticity or absorption were measured).

The goal of data analysis was the calculation of distribution diagrams and pure (individual) spectra for all *nc* components considered throughout the process. The distribution diagram provides information about the stoichiometry and stability of the acid-base components

considered. In addition, the shape and intensity of the pure spectra may provide qualitative information about the structure of those components.

For acid-base experiments the model will include a set of chemical equations describing the formation of the different acid-base components from the neutral species, together with approximate values for the stability constants, such as the following:

$$DNA + pH^{+} \leftrightarrow DNA{\cdot}H_p \; Beta_{1p} = [DNA{\cdot}H_p]/[DNA]\,[H^{+}]^{p} \quad (4)$$

In this equation, the parameter *p* is related to the Hill coefficient and describes qualitatively the cooperativity of the equilibrium. Values of *p* >1 indicate the existence of a cooperative process.

Whenever a physico-chemical model is applied, the distribution diagram in **C** complies with the proposed model. Accordingly, the proposed values for the equilibrium constants and the shape of the pure spectra in $\mathbf{S}^{\mathbf{T}}$ are refined to explain satisfactorily data in **D**, whereas residuals in **E** are minimized. In this study, hard-modeling analysis of acid-base experiments used the EQUISPEC program [27]. This approach has been used previously to characterize pH-induced transitions in i-motif structures found near the promoter regions of the n-myc [28], and SMARCA4 genes [29], among others.

2.3.3. DNA:ligand titrations

The determination of the ratio ligand:DNA and the calculation of the binding constants were conducted from the fluorescence data recorded along titrations of ligands with DNAs by using the Equispec program, as described elsewhere [30].

3. Results and discussion

3.1. In silico prediction of folded structures

All sequences, except IDJ1noduplex, may adopt hairpin structures at pH 7.0, 50 mM Na^{+} and 14 °C, according to Nupack calculations [31]. The expected hairpins are shown in Fig. S1. More importantly, these sequences may form hybrid i-motif/duplex structures. A preliminary value of the propensity to the formation of i-motif structures was calculated by means of G4Hunter, despite this method being mostly parametrized for the prediction of G-quadruplex structures [32]. As expected, all these sequences show a tendency to the formation of i-motif structures (Fig. S2).

3.2. Melting experiments

First, melting experiments were carried out at pH 5.2 and 7.4 to characterize the stability of the folded structures. Fig. 2 shows the normalized absorbance values measured at 260 nm. Tables 2 and 3 summarize the thermodynamic parameters calculated from these melting traces. The changes in enthalpy and entropy have been considered constant within this range of temperatures.

Meltings done at pH 5.2 showed only one transition around 55–60 °C (Fig. 2a). The i-motif formed by the IDJ1 sequence unfolded with a T_m value equal to 58.9 ± 0.5 °C (Table 2). Removal of the duplex or G:T:G:T tetrad moieties produced a decrease in the value of T_m. Surprisingly, removal of the T·T base pair produced a slight increase of the T_m value, that could be related to changes in the loops [3]. However, according to the cooperativity of the transition, i.e., to the value of Gibbs free energy at 37 °C, the most stable structure at this temperature is that adopted by IDJ1. The changes in enthalpy and entropy associated to the folding of the i-motif structures adopted by IDJ1noduplex, IDJ1notetrad, and IDJ1noTs were similar (considering the associated uncertainties), but smaller than in the case of IDJ1. This fact suggested a lower stability of the i-motif at pH 5.2 and 37 °C when the duplex, G:T:G:T or T:T moieties were removed.

At pH 7.4, the plot is different from that shown at pH 5.2. For IDJ1, two transitions were observed at 260 nm. This observation agrees with that previously reported [14], and it was related to the unfolding of the i-motif and duplex moieties at 15.9 ± 1.0 and 57.6 ± 0.6 °C, respectively. Complementary melting experiments with the duplexIDJ1 sequence, that only may form duplex structures, showed a T_m value around 64 °C (data not shown). The lowest value of the T_m value corresponding to the

Table 2
Thermodynamic parameters related to the folding of the i-motif structures at pH 5.2 (20 mM acetate buffer). A two-state process was considered in the calculations. Two replicates were done in each case. The values given correspond to the average and standard deviation.

DNA sequence	ΔH (kcal·mol^{-1})	ΔS (cal·K^{-1}·mol^{-1})	ΔG_{37} (kcal·mol^{-1})	T_m (°C)
IDJ1	−92 ± 4	−276 ± 11	−6.0 ± 0.4	58.9 ± 0.5
IDJ1noduplex	−72 ± 16	−220 ± 49	−4.1 ± 1.0	55.8 ± 0.1
IDJ1notetrad	−72 ± 9	−219 ± 26	−4.0 ± 0.3	55.5 ± 0.9
IDJ1noTs	−58 ± 4	−176 ± 13	−4.3 ± 0.3	61.9 ± 0.2

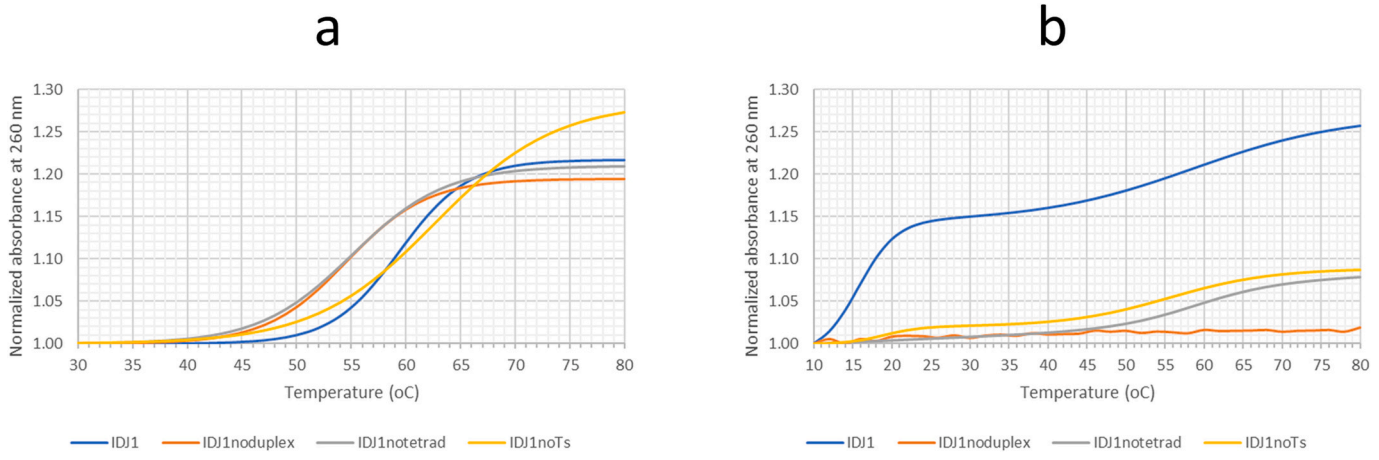

Fig. 2. Normalized absorbance values measured at 260 nm, at pH 5.2 (a) and 7.4 (b). The experimental conditions were 20 mM phosphate or acetate buffer, and 2 micromolar DNA concentration. The graphs show the calculated melting curves from the thermodynamic parameters given in Tables 2 and 3, which in turn correspond to the average values of, at least, two independent melting experiments.

Table 3
Thermodynamic parameters related to the folding of the folded structures at pH 7.4 (20 mM phosphate buffer). A minimum of three replicates were done in each case. The values given correspond to the average and standard deviation.

DNA sequence	First transition				Second transition			
	ΔH (kcal·mol^{-1})	ΔS (cal·K^{-1}·mol^{-1})	ΔG_{37} (kcal·mol^{-1})	T_m (°C)	ΔH (kcal·mol^{-1})	ΔS (cal·K^{-1}·mol^{-1})	ΔG_{37} (kcal·mol^{-1})	T_m (°C)
IDJ1	−63 ± 17	−217 ± 59	4.6 ± 1.3	15.9 ± 1.0	−29.6 ± 8.6	−89.6 ± 26.1	−1.8 ± 0.5	57.5 ± 0.6
IDJ1noduplex	–	–	–	<10	–	–	–	–
IDJ1notetrad	–	–	–	<10	−42.7 ± 1.3	−128.6 ± 3.9	−2.8 ± 0.1	58.8 ± 0.5
IDJ1noTs	−44 ± 10	−151 ± 34	3.4 ± 0.1	15.4 ± 1.0	−33.0 ± 2.9	−99.2 ± 8.3	−2.2 ± 0.3	58.8 ± 1.3
duplexIDJ1					−34 ± 2.5	−100.8 ± 7.6	−2.7 ± 0.5	64.4 ± 0.5

unfolding of the duplex moiety in IDJ1 in relation to that in the duplex structure adopted by the duplexIDJ1 sequence was related to the presence of the long strand resulting from the melting of the i-motif in IDJ1, which is not present in duplexIDJ1.

The melting of the IDJ1noduplex sequence did not show any clear transition at 260 nm, which suggests a low stability of the i-motif and duplex moieties at this pH value. In other words, the lack of a relatively large duplex moiety hinders the formation of a stable i-motif. The melting of the IDJ1notetrad sequence shows a clear sigmoidal transition at 58.8 ± 0.5 °C, which is related to the unfolding of the duplex moiety. A transition at lower temperatures, which could be related to the i-motif moiety, was not observed clearly. Finally, the melting of the IDJ1noTs sequence showed again two transitions at 15.4 ± 1.0 and 58.8 ± 1.3 °C, which could be related to the unfolding of the i-motif and duplex moieties, respectively. Therefore, the removal of the T:T base pair produced a smaller destabilizing effect on the whole structure than the removal of the duplex or of the G:T:G:T tetrad moieties.

Complementary melting experiments monitored with circular dichroism spectroscopy were carried out at pH 7.4. At 5 °C, the CD spectrum of IDJ1noduplex (Fig. 3b) showed a positive signal around 275 nm, which is compatible with a partially stacked strand. The CD spectra of IDJ1notetrad (Fig. 3c) and IDJ1noTs (Fig. 3d) showed a negative signal at 250 nm, and positive signals at 220 and 280 nm. These spectral features are compatible with a B-DNA conformation. Finally, the CD spectrum of IDJ1 shows a negative signal at 250 nm, positive signals at 220 and 280 nm, and a shoulder around 290 nm (Fig. 3a). The positive contribution around 290 nm in the spectrum of IDJ1 would agree with the presence of the i-motif moiety, the CD spectrum of which shows a characteristic positive band around 285–288 nm [33].

The spectral changes observed along the melting of IDJ1 pointed out to the existence of more than one transition (Fig. 3e). This fact agrees with the two transitions observed in Fig. 2b. For IDJ1noduplex, a sharp transition is observed at very low temperatures, making not possible the determination of the melting temperature without a great uncertainty. This also agrees with the previous melting experiments monitored with absorption spectroscopy. In the case of IDJ1notetrad and IDJnoTs, the unfolding of the duplex moiety is clearly observed at high temperatures, whereas the unfolding of the i-motif moiety, despite being not as obvious as that of the duplex, can be observed at low temperatures.

Multivariate analysis was applied to analyze the set of CD spectra

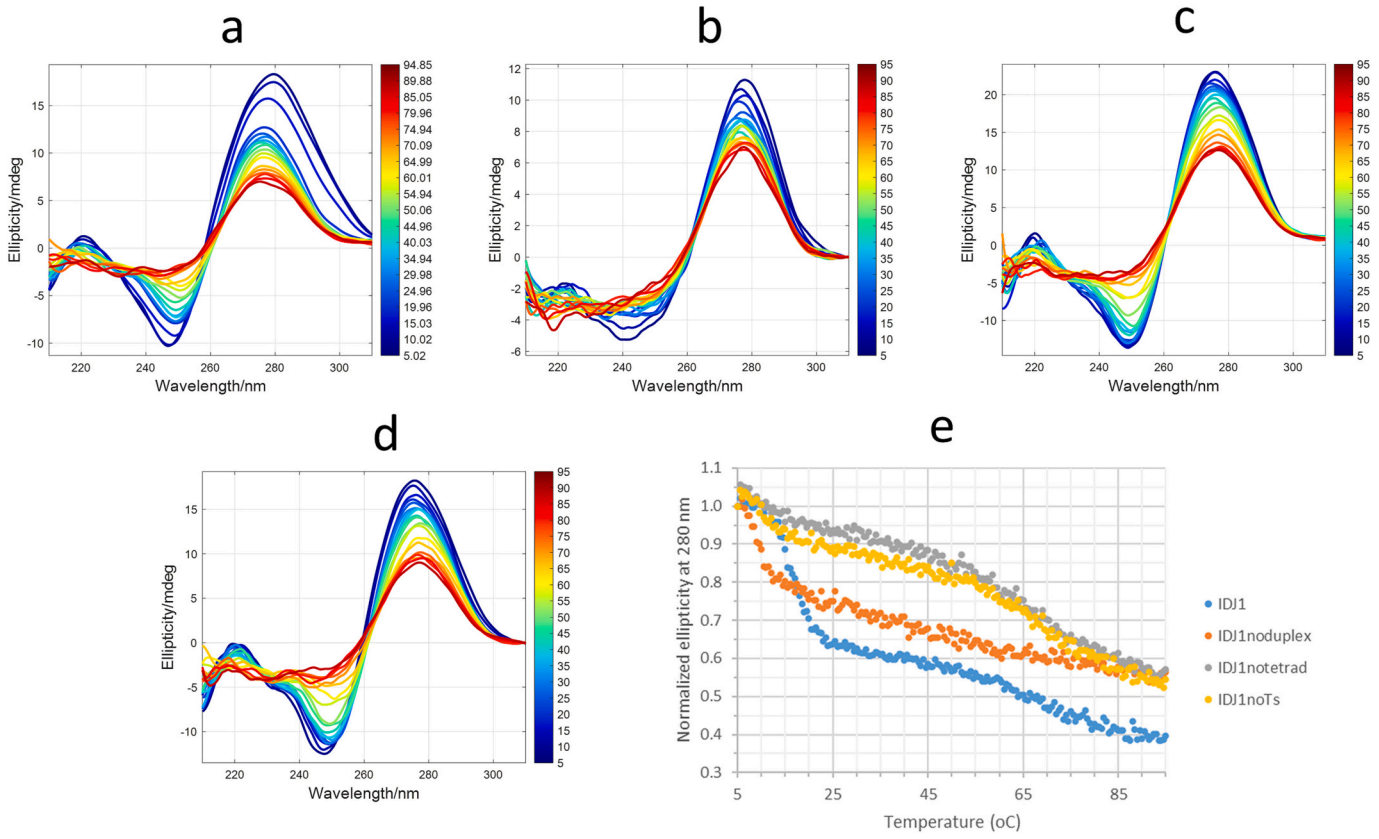

Fig. 3. CD spectra measured along the meltings of IDJ1 (a), IDJ1noduplex (b), IDJ1notetrad (c), and IDJ1noTs (d), and ellipticity values recorded at 280 nm (e). The experimental conditions were 2 μM DNA concentration, 20 mM phosphate buffer, pH 7.4.

shown in Fig. 3a-d. For IDJ1, the analysis demonstrated the presence of two transitions [26]. The calculated distribution diagram and pure spectra for each one of the three proposed species is given in Fig. 4a and e, respectively. The corresponding lack-of-fit is shown in Fig. S3. The species depicted in blue corresponds to the initial i-motif/duplex structure (Fig. 4a). The resolved pure CD spectrum for this species (Fig. 4e, blue) shows a shape that resembles that of a B-DNA structure with an additional positive ellipticity around 290 nm that was related to the presence of the i-motif moiety. Upon heating, this initial conformation unfolds cooperatively to yield the species colored in red (Fig. 4a), which was related to the structure lacking the i-motif moiety. The CD spectrum of this species (Fig. 4e, red) is very similar to that of B-DNA. Upon heating, a smooth transition is observed to yield the species colored in yellow (Fig. 4a), that according to the resolved CD spectrum (Fig. 4e, yellow) would correspond to the unfolded strand.

A similar model of three species was proposed for the unfolding of IDJ1noTs (Fig. 4d and h), which agrees with the previous melting experiments monitored with absorption spectroscopy. It must be pointed out the difference in the sharpness of the transition from the initial i-motif/duplex structure (blue) to the duplex (red) in comparison with that observed for IDJ1. This confirms that the T:T base pair play a certain role in the stabilization of the i-motif, despite being minor than that of the duplex or the G:T:G:T tetrad.

In the case of IDJ1noduplex, only two species were considered, and a smooth transition related to the unfolding of a partially stacked structure (Fig. 4b and f, green) to yield the unfolded (Fig. 4b and f, yellow) was modelled. Finally, the unfolding of IDJ1notetrad was also modelled with two components. According to the spectral features of the resolved spectrum, the initial species (Fig. 4c and g, red) would correspond to the duplex structure lacking the i-motif moiety. Upon heating, a smooth transition will yield the unfolded strand (Fig. 4c and g, yellow). However, the lack-of-fit shows that this model of two species, i.e., only one transition, does not explain the subtle variation of ellipticity at 280 nm at low temperatures (Fig. S3c). This indicates a minor presence of the i-motif/duplex structure at low temperatures. We have tried to fit a three-species model, i.e., two transitions (like Fig. 4a and e), to this data set, but it was not possible to achieve a reliable mathematical resolution of the very minor contribution of the hybrid i-motif/duplex structure at 5 °C.

3.3. Acid-base titrations

To have a more detailed description of the major species at neutral pH and of their acid-base properties, spectroscopically monitored titrations were carried out. As example, Fig. 5a shows the CD spectra recorded along the acid-base titration of IDJ1 at 20 °C, whereas Fig. 5b shows the ellipticity changes at 280 nm recorded along this titration. In this case, at least two pH-induced transitions were observed, at pH values around 7.4 and 4.5, which would involve the existence of, at least, three different acid-base species. Similar data sets were obtained for the other sequences studied in this work.

For each titration, the set of CD spectra recorded was examined by means of a multivariate data analysis method based on the previous proposal of a model of acid-base species and pH-induced transitions. Previous works have shown the application of this methodology to the analysis of acid-base and ligand:DNA interaction equilibria involving both i-motif and G-quadruplex structures [30,34]. The model is characterized by the number of acid-base species, the value of the $pH_{1/2}$ that determines the transition between two structures, and a parameter related to the cooperativity of the transition.

The results obtained with this methodology are summarized in Table 4. For all titrations, four acid-base species, i.e., three pH-induced transitions, were needed to fit the experimental data. However, the nature of each one of the acid-base species and the values of $pH_{1/2}$ at which evolve one species into another are different depending on the considered sequence. The corresponding lack of fit, i.e., a measure of the goodness of the proposed model, is shown in Fig. S4.

For IDJ1, the calculated concentration profiles for the four species considered are shown in Fig. 5c. The first pH-induced transition is characterized by a $pH_{1/2}$ value of 7.51 ± 0.10 (Table 4), which corresponds to the transition from the major species at neutral pH values (depicted in blue) to the first protonated species (red). The nature of these species may be deduced from the observation of Fig. 5d, and from the previous information gained from melting experiments. For IDJ1 (Fig. 5d, blue line), the calculated spectrum for the neutral species at 20 °C shows a strong positive band at 275 nm, a weak band around 220 nm, and a negative signal at 250 nm. This signature is mostly compatible with a double stranded B-DNA. Hence, it should correspond to the partially unfolded structure where the i-motif has been already lost. The

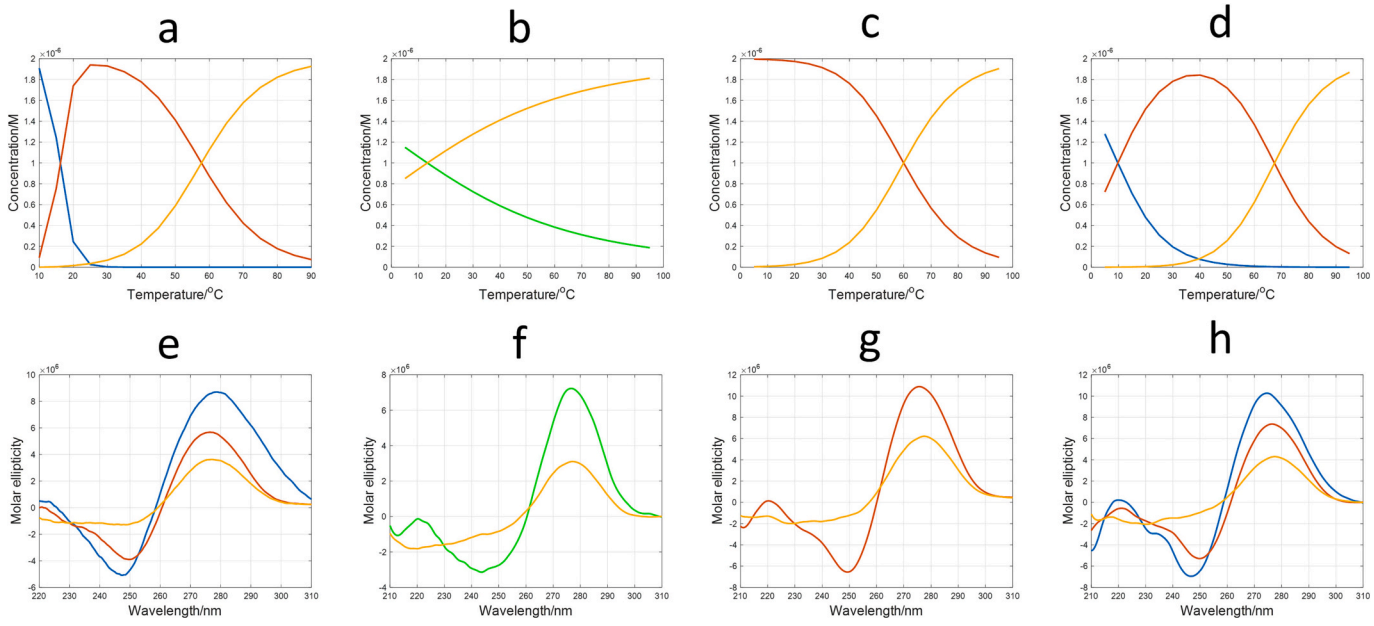

Fig. 4. Distribution diagram and pure CD spectra calculated with multivariate analysis from the spectra recorded along CD-monitored melting experiments of IDJ1 (a, and e), IDJ1noduplex (b, and f), IDJ1notetrad (c, and g), and IDJ1noTs (d, and h). The blue, red, green, and yellow colors represent the initial i-motif/duplex structure, the duplex structure, the partially stacked strand, and the unfolded strand, respectively.

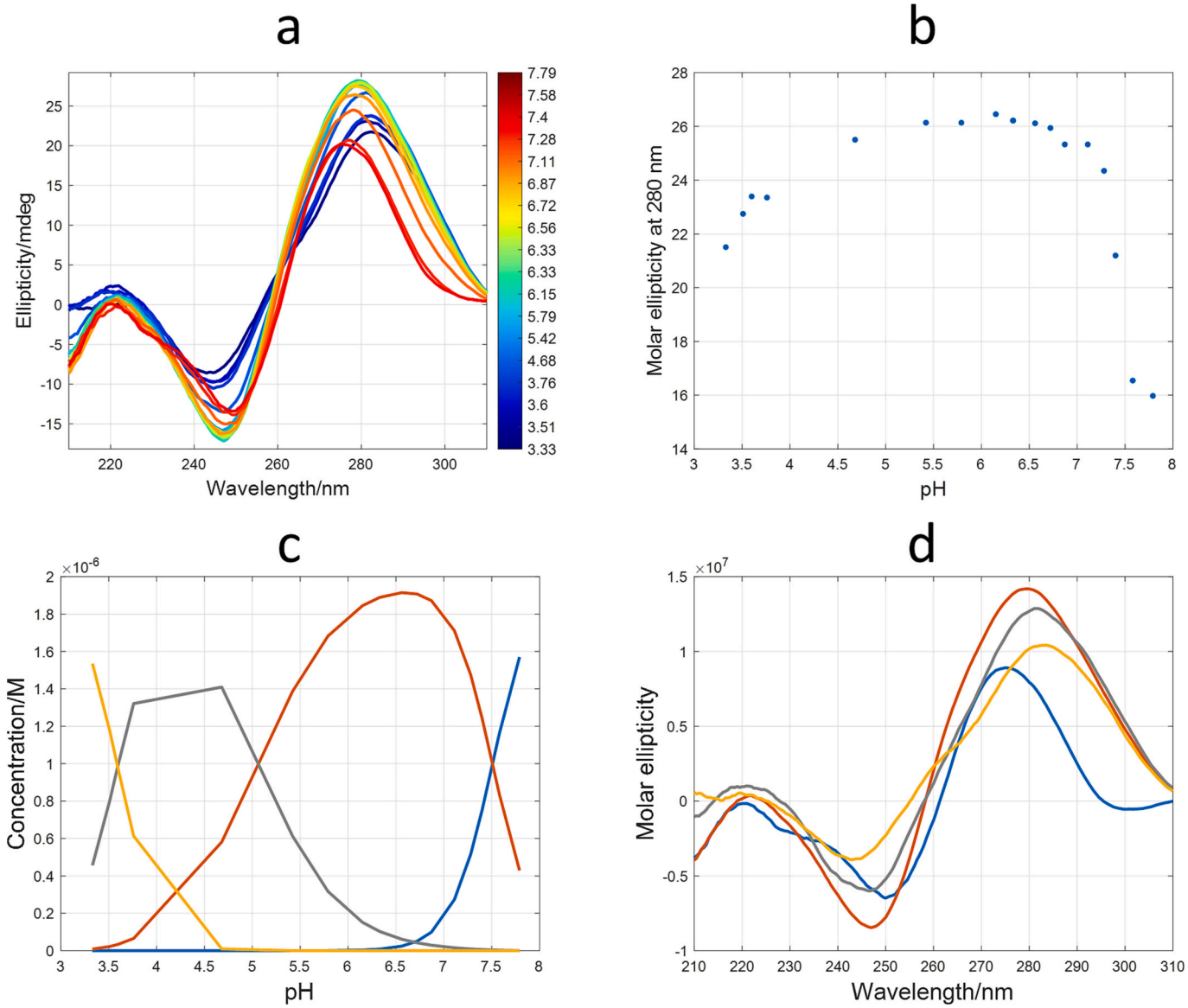

Fig. 5. Acid-base titration of IDJ1 at 20 °C. (a) CD spectra measured along the titration. Numbers at right represent the pH values at which spectra were measured. (b) Variation of ellipticity measured at 280 nm vs. pH. The experimental conditions were 2 μM DNA concentration, 20 mM phosphate buffer, pH 7.4. (c) Calculated concentration profiles from the multivariate analysis of CD spectra recorded along the acid-base titrations of IDJ1. (d) Calculated pure spectra for each one of the acid-base species shown in panel c.

Table 4
Parameters characterizing the acid-base distribution diagrams of the studied DNAs. The parameters $pH_{1/2}$ and p explain the midpoint of the corresponding transition, and its cooperativity, respectively. Values of $p > 1$ indicate the existence of a cooperative process. The spectroscopically monitored titrations were carried out at 20 °C, 20 mM phosphate buffer.

DNA sequence	First transition		Second transition		Third transition	
	$pH_{1/2}$	p	$pH_{1/2}$	p	$pH_{1/2}$	p
IDJ1	7.51 ± 0.10	3	5.26 ± 0.17	1	3.59 ± 0.24	2
IDJ1noduplex	6.62 ± 0.16	3	5.10 ± 0.44	1	3.06 ± 0.43	2
IDJ1notetrad	6.55 ± 0.10	3	4.76 ± 0.10	1	3.43 ± 0.12	2
IDJ1noTs	6.75 ± 0.09	3	4.54 ± 0.10	1	2.87 ± 0.30	2
duplexIDJ1	–	–	4.79 ± 0.07	1	3.73 ± 0.10	1

CD spectrum of the second acid-base species (Fig. 5d, red line) shows similar trends to those of the neutral species, but the position of the bands has been shifted. These signatures are compatible with the formation of the hybrid i-motif/duplex structure.

The $pH_{1/2}$ value for the second pH-induced transition was 5.26 ± 0.17 (Table 4 and Fig. 5c). It was related to a transition between two different i-motif structures (depicted in red and grey, respectively). The shape of the resolved CD spectra (Fig. 5d, red and grey lines, respectively) is very similar.

Finally, the third transition was characterized by a value of $pH_{1/2}$ equal to 3.59 ± 0.24 (Table 4 and Fig. 5c). It was related to the transition from the second i-motif (grey) to the fully protonated species (yellow). This assignment is clear as the calculated spectrum for the fully protonated species shows the characteristic signature of unfolded DNA sequences (Fig. 5d, yellow line).

As for comparison, the acid-base titration of the duplexIDJ1 sequence was also carried out (Fig. S5). This sequence only shows the duplex-forming moiety, and it is expected not to form any i-motif structure. The analysis of CD spectra recorded from pH 7.7 to 3.0 was explained with three species. The first one was related to the initial duplex structure present at pH 7.7. Two $pH_{1/2}$ were determined, with

values equal to 4.79 ± 0.01 and 3.73 ± 0.10. These values have been related to the protonation of cytosine and adenine bases, respectively.

The titration shown in Fig. 5 was carried out at 20 °C. Therefore, a different concentration profile would be expected if the titration was done 37 °C. Fig. S6 shows the CD spectra measured along the titration, as well as the results of the multivariate analysis. As expected from the melting experiments of the IDJ1 described above, the stability of the hybrid i-motif/duplex structure is lower at 37 than at 20 °C. This fact is reflected in the pH ranges where each species predominates. At 37 °C, the value of the $pH_{1/2}$ that determines the formation of the i-motif from the neutral species has been shifted from 7.51 ± 0.10 (at 20 °C) to 6.59 ± 0.06 (at 37 °C).

The resolved distribution diagrams and pure spectra for the other sequences are given in Fig. S7 and S8. In Table 4, it can be observed that the value of the *p* value for the first pH-induced transition is greater (3) than for the second and third transitions (1 and 2, respectively). This was related to the strong cooperativity of the transition from the major species at neutral pH (blue in Fig. 5) to the first i-motif (red in Fig. 5). On the other hand, the value of $pH_{1/2}$ for this first transition is greater for IDJ1 than in the other cases. On the contrary, the lower values of $pH_{1/2}$ for this first transition were obtained for IDJ1notetrad and IDJ1noduplex. All these observations may be explained by the strong stabilization of the i-motif structure when all the considered moieties (duplex, G:T:G:T tetrad, and T:T base pair) are present. The removal of T:T base pair produces a clear destabilization of the i-motif, but lower than in the cases of G:T:G:T tetrad or duplex.

The value of $pH_{1/2}$ related to the second transition is near the pK_a of free cytosine (4.5 at 25 °C). Also, the value of the p parameter for this second transition reflects its small cooperativity. These observations would agree with the protonation of cytosines not participating in the core of the i-motif, and with the small conformational changes on the i-motif in this pH range, as described previously.

Finally, the value of $pH_{1/2}$ related to the third transition is smaller than the pK_a of free cytosine and slightly higher than the pK_a of guanine. Also, the value of the p parameter for this third transition reflects a certain cooperativity, which agrees with the unfolding of the i-motif structure to yield the fully protonated species. Overall, the lowest value of the $pH_{1/2}$ in relation to that of free cytosine and the relatively high cooperativity related to this transition may be all explained because they reflect the protonation of cytosines involved in the i-motif core, which are much more difficult to protonate than other cytosines, and subsequent unfolding. The values of $pH_{1/2}$ are greater for IDJ1 and IDJ1notetrad, and small for IDJ1noduplex and IDJ1noTs. This means that the i-motif formed by IDJ1noTs is the most stable upon protonation.

3.4. Interaction with ligands

As commented before, searching for selective i-motif binders that could enhance its stability at biological conditions of pH and temperature has been done extensively [35,36]. In this work, the interaction of IDJ1 with several molecules has been studied (Fig. 1).

The CD spectra in the UV region of the 1:3 (DNA:ligand) mixtures at pH 7.4 are shown in Fig. S9. Any structural changes were observed. In addition, no induced CD signal was observed in the visible region for any of the mixtures.

Melting experiments were carried out for 1:3 (DNA:ligand) mixtures. Table 5 summarizes the values of the determined T_m values. The shift of the melting temperature of IDJ1 in presence of the ligands was very small or null for all the mixtures. It was observed that some ligands stabilized the duplex moiety, whereas little interaction was observed with the i-motif part (Fig. 6a). This agrees with previous observations on the destabilization of i-motif structures by stablished G-quadruplex ligands [37]. Indeed, the stabilization of i-motif structures by proposed binders has been put into question recently [9].

PAGE experiments were also carried out (Fig. 6b). IDJ1 (lane 2) ran slower than IDJ1noduplex (lane 3) in concordance with its higher ordered structure. In addition, the staining was different for IDJ1 giving a darker band also suggesting that the oligonucleotide was not in a single stranded form as for IDJ1noduplex. Previously studies have demonstrated that stains-all gives a light blue colour when intercalated in single-stranded oligonucleotides and a darker one when intercalated in double-stranded or more structured motifs [38]. For the mixtures of IDJ1 with the different dyes (lane 4 to 10) the apparition or shift of different bands was not observed, indicating that the addition of the ligands could not trigger any conformational change or formation of different structures at these conditions.

Fluorescence-monitored titrations involving IDJ1, IDJ1noduplex, and duplexIDJ1 with BA41 were carried out at 10 °C and pH 7.4. BA41 shows weak green fluorescence when excited at 365 nm. When BA41 was titrated with IDJ1noduplex, which lacks ordered structure, the fluorescence signal did not show any variation at 517 nm (Fig. 7a). On the contrary, the titration of BA41 with duplexIDJ1 produced a 75 % of reduction of the initial fluorescence. An additional 15 % of reduction was observed when BA41 was titrated with IDJ1. These changes suggest that the strongest interaction happens with the duplex moiety of IDJ1.

The spectra measured along the titrations were examined by means of the multivariate data analysis method previously described in the study of the pH-induced transitions. For the titration of BA41 with duplexIDJ1, a 1:2 (DNA:ligand) stoichiometry was proposed (log binding constant was equal to 12.4 ± 0.2, Fig. S10). A similar approach was tried to fit the spectra measured along the titration of BA41 with IDJ1. However, in this case it was not possible to determine a definite stoichiometry. The model consisting of a 1:2 stoichiometry did not fit satisfactorily the data, probably because of the presence of additional non-specific interaction with the i-motif moiety of the structure. Inverse titrations where the DNA was titrated with the ligand were also carried out (Fig. 7b). In agreement with the direct titrations, addition of BA41 to IDJ1noduplex produced a clear increase of the fluorescence related to

Table 5
Melting temperatures of 1:3 mixtures of IDJ1 and selected ligands. Meltings were done at pH 7.4 (20 mM phosphate buffer).

Ligand	First transition				Second transition			
	ΔH (kcal·mol^{-1})	ΔS (cal·K^{-1}·mol^{-1})	ΔG_{37} (kcal·mol^{-1})	T_m (°C)	ΔH (kcal·mol^{-1})	ΔS (cal·K^{-1}·mol^{-1})	ΔG_{37} (kcal·mol^{-1})	T_m (°C)
IDJ1 – no ligand	−63	−217	4.6	15.9	−29.6	−89.6	−1.8	57.5
MK4827	−67	−232	4.9	15.8	−20.8	−62.9	−1.3	57.4
Curaxin	−89	−308	6.5	16.0	−35.5	−108.4	−1.9	54.2
LOM1392	−81	−279	6.1	15.2	−21.7	−65.3	−1.4	59.0
ABT888	−85	−294	6.3	15.8	−27.3	−83.2	−1.5	55.0
BA41	−57	−200	4.3	15.6	−44.3	−133.8	−2.8	57.6
Quercetin	−78	−272	6.2	14.3	−23.1	−70.5	−1.2	54.1
Resveratrol	−119	−415	9.4	14.5	−20.6	−61.7	−1.5	61.0
TMPyP4	−80	−279	6.7	13.1	−16.1	−48.5	−1.0	58.0
Sinapic acid	−72	−251	5.9	13.7	−20.6	−62.1	−1.4	59.0
(+)-Catechin	−73	−256	6.0	13.5	−29.5	−89.2	−1.8	57.3
Palmatine	−91	−315	6.1	17.5	−18.4	−56.2	−1.0	54.6

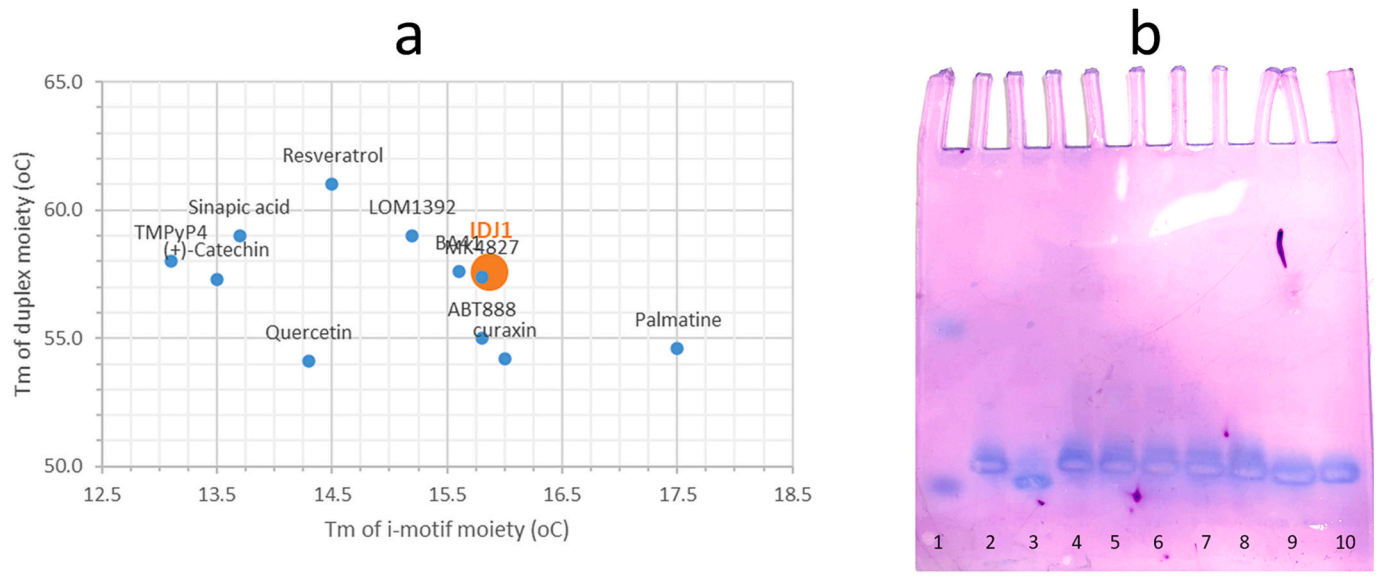

Fig. 6. (a) T_{m2} vs. T_{m1} for DNA:ligand mixtures (1:3). The orange circle represents the values for IDJ1. (b) PAGE. 1: Bromophenol blue/Xylene cyanol, 2: IDJ1, 3: IDJ1noduplex, 4: Sinapic acid:IDJ1 (3:1), 5: Quercetin:IDJ1 (3:1), 6: (+)-Catechin:IDJ1 (3:1), 7: Resveratrol:IDJ1 (3:1). 8: TMPyP4:IDJ1 (3:1), 9: Palmatine:IDJ1 (3:1), 10: Palmatine:IDJ1 (6:1).

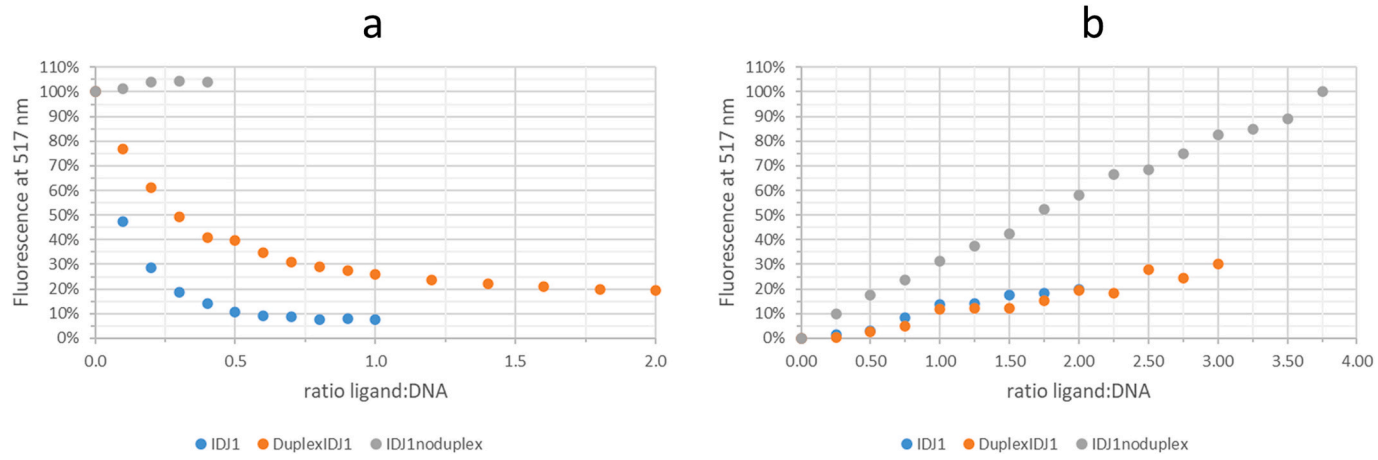

Fig. 7. Interaction of BA41 with several sequences monitored by molecular fluorescence spectroscopy. (a) Titrations of the ligand with DNAs. (b) Titration of DNAs with the ligand. The experimental conditions were 2 μM DNA concentration, 20 mM phosphate buffer, 10 °C, pH 7.4.

the unbounded ligand, whereas quenching was observed for the other two sequences.

NMR was used to study the interaction of BA41 with IDJ1. The oligonucleotide IDJ1 displayed a high-quality ^{1}H NMR spectrum and the signals have been attributed following the assignments already reported in literature [14]. As reported, narrow and well-resolved imino protons are present in the ^{1}H NMR spectrum, which are consistent with the identification of the hybrid structure i-motif/duplex. Imino resonances corresponding to C:C$^+$ (15–16 ppm), Watson-Crick (12.5–14.0 ppm) base –pairs and G:T or T:T mismatches were observed (Fig. 8).

Following the imino proton signals during the titration experiment with BA41 till ratio R = [BA41]/[IDJ1] = 3.0, no significant changes in the imino protons corresponding to i-motif were observed. On the contrary an important line broadening of the signals attributed to NH imino protons corresponding to the residues in the duplex moiety were detected. The same behavior could be observed for the residues G4 and G29 belonging to the G:T:G:T tetrad and for the T35 of T:T base pairs. This suggested that these NH imino protons experienced a different molecular environment, most likely due to non-specific ionic interactions with the ligand mainly with the duplex moiety. The junction and the G:T:G:T tetrad are also involved in the binding whereas no binding is observed for i-motif structure confirming our fluorescence and CD results.

4. Discussion

There is a growing interest in the study of the regions of the genome where it is possible to find nearby secondary structures of a different nature (duplex, i-motif, G-quadruplex…) [39]. These regions could promote selective binding sites that, upon interaction with the appropriate ligand, would modify the stability of these structures [40]. Concerning the i-motif, it is known that its stability at neutral pH and 37 °C is rather low, and effort is being done in the research of proteins and natural or synthetic ligands that could increase it. In this sense, the existence of these junctions could be a tool to modulate the stability of the i-motif structure in vivo.

In a recent work, the structure adopted by the IDJ1 sequence at pH 7 was determined [14]. This structure may be viewed as an i-motif stabilized by an internal duplex (i.e., an internal hairpin), a G:T:G:T tetrad, and a T:T base pair. Hence, several junctions may be considered within

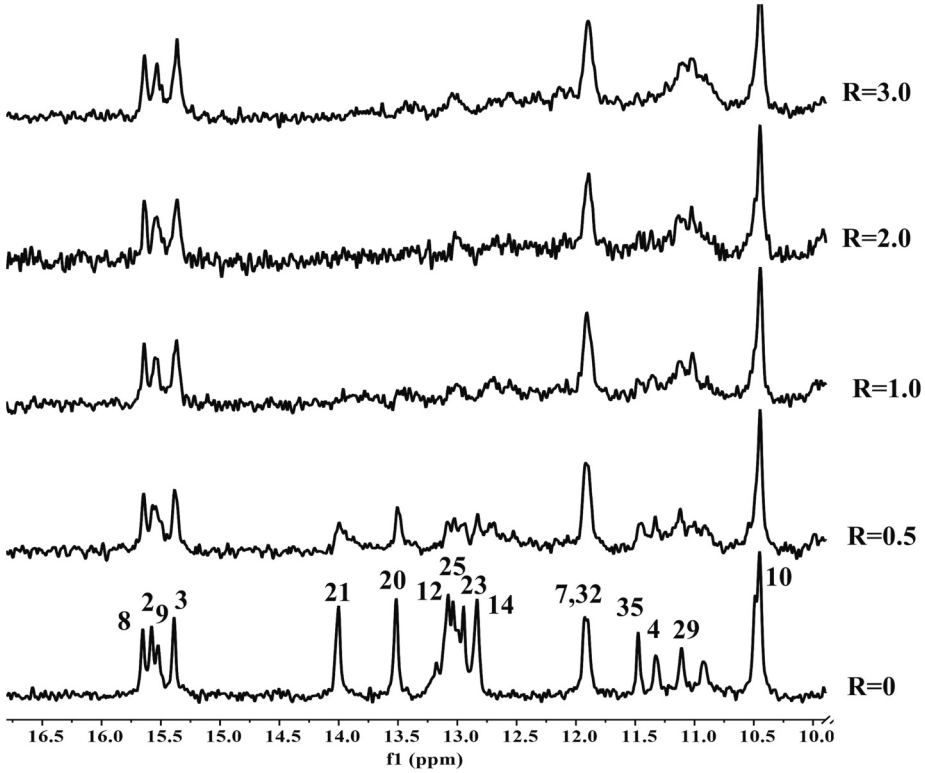

Fig. 8. Imino protons region of ^{1}H NMR spectra acquired at 5 °C, (H_2O/D_2O 9:1) buffer solution 20 mM potassium phosphate buffer, pH 7.4, of IDJ1 in presence of BA41 at different ratios R = [drug]/[DNA].

this structure. In the present work, the role of each one of these three structural motifs on the overall thermodynamic stability of the i-motif has been studied at pH 5.2 and 7.4. Spectroscopic and chemometric methods have been used with this purpose.

At neutral pH, it has been shown here that the most important element contributing to the thermal stability of the i-motif are the duplex and the G:T:G:T tetrad. Without these moieties, the i-motif is only formed at pH 7.4 at very low temperatures. Finally, the removal of the T:T base pair, whereas affecting to the stability of the i-motif, does not prevent its formation.

To have a more detailed picture of the effect of these structural motifs on the acid-base properties of IDJ1, spectroscopically monitored acid-base titrations of the mutated sequences were done. The results have highlighted again the stabilizing effect of the duplex and of the G:T:G:T tetrad on the pH-induced folding of IDJ1. In this sense, the application of multivariate analysis has allowed the determination of the number of pH-induced transitions, their degree of cooperativity, as well as the concentration profiles and pure spectra corresponding to each one of the species present in the pH range considered. As example, this approach has allowed the resolution of two different i-motif species, as it has also been shown recently by Amato et al. for the equilibria involving i-motif and hairpin species [41] . The existence of two slightly different i-motif structures has been proposed previously for cytosine-rich sequences based on the telomeric sequence [19,28,29,42]. In these early works, this transition was hypothesized to be related with the additional protonation of cytosine bases located at the loops of the i-motif, and which did not participate into the core of the i-motif. Very recently, the atomistic nature of this transition has been explained for a given sequence by using NMR and modeling tools in terms of base pairing and specific loop motions near the pK_a of cytosine [43,44].

As commented above, the interaction with ligands could be a tool to increase the stability of i-motif structures. Unfortunately, despite many articles claiming the discovery of selective ligands with i-motif structures [45,46], it is not clear how selective are these. It seems that non-selective, electrostatics interaction could be behind the reported interactions of ligands with i-motif structures, as most of these ligands hardly affect the T_m values of the considered structures [9]. In this sense, the existence of additional structural motifs, such as hairpins, could be a way to increase the stability of i-motif structures. In this work, the interaction of IDJ1 with several ligands has been studied.

The results have shown that, despite a certain stabilization of the duplex moiety, little stabilizing interaction with the i-motif has been observed at pH 7.4 and 25 °C. Five ligands that have been reported to stabilize G-quadruplex structures were studied, including BA41. The NMR study of the interaction of this ligand with IDJ1 revealed that that the strongest interaction occurs with the duplex moiety of IDJ1, whereas no interaction was observed for the i-motif moiety. Concerning the polyphenols considered in this work, the interaction of fisetin, another polyphenol, with several i-motif structures has been recently studied [47–49]. The fluorescence and CD spectra recorded along the titrations of fisetin with the i-motif adopted by the VEGF sequence at pH 5.4 and 25 °C, were explained because of the ligand-induced transition from the initial i-motif to a hairpin structure. Surprisingly, other i-motif structures did not produce spectral changes in a similar way to VEGF. These observations pointed out to the role of the bases at the loops on the interaction of this ligand with i-motifs. Concomitantly with the previous work, the interaction of fisetin and quercetin with an i-motif-forming sequence found near the promoter region of the *bcl-2* gene has been studied by means of mass spectrometry [47]. At pH 7, the proposed stoichiometry DNA:ligand was 1:1, and the calculated binding constants were around 10^4 M^{-1}. This low value of the constant indicates a very weak binding of the ligand to the structure adopted by the sequence at this pH, presumably a hairpin.

Previous reports have shown that palmatine, an alkaloid, interacts with duplex or G-quadruplex structures, but rather weak with i-motifs [17]. In the present work, little interaction has been observed. Also, the interaction of TMPyP4 with i-motifs structures has been studied. In a pioneer work, Fedoroff et al. proposed that two TMPyP4 molecules stack

on the terminal C·C$^+$ base pairs of a tetramolecular i-motif [46]. Recently, Alniss et al. studied the interaction of TMPyP4 with a long G,C-rich oligonucleotide, prone to form hairpin structures at neutral pH, by means of CD and ITC. The results were explained as a result of the interaction of the molecule in a 1:1 (DNA:ligand) or 1:2 stoichiometry, depending on the sequence studied [50]. Because no thermal data were provided, it is difficult to assess the stabilizing effect of TMPyP4 on i-motif structures. In our work, however, we have not observed a clear stabilization of the structure adopted by IDJ1 at neutral pH by interaction with TMPyP4.

5. Conclusions

In this work, it has been assessed that the duplex moiety is the most important contribution to the thermal stability of the i-motif formed by IDJ1 at pH 7.4. The second most important contribution is the G:T:G:T tetrad, and residual stabilization is provided by the T:T base pair. Spectroscopically monitored acid-base titrations and multivariate analysis allowed a detailed description of the pH-induced conformational equilibria in these sequences. It was observed that the addition of the duplex moiety greatly shifts the $pH_{1/2}$ of i-motif structure, providing additional stability at neutral pH. Unfortunately, no special stabilization of this hybrid i-motif/duplex structure was observed upon interaction with the considered ligands.

CRediT authorship contribution statement

Judit Rodriguez: Investigation, Formal analysis. **Arnau Domínguez:** Investigation, Formal analysis. **Anna Aviñó:** Investigation, Resources, Writing – review & editing. **Gigliola Borgonovo:** Investigation, Formal analysis. **Ramon Eritja:** Conceptualization, Methodology, Resources, Writing – review & editing, Funding acquisition. **Stefania Mazzini:** Investigation, Formal analysis, Writing – review & editing, Funding acquisition. **Raimundo Gargallo:** Conceptualization, Methodology, Software, Writing – review & editing, Supervision, Project administration.

Declaration of competing interest

The authors declare that they have no known competing financial interests or personal relationships that could have appeared to influence the work reported in this paper.

Acknowledgements

Aina Aguilera is thanked for carrying out some of the experiments shown here during her stay at the UB in the framework of a program to promote scientific careers. Dr. Óscar Núñez (UB) is thanked for providing the polyphenols studied in this work. Funding from Spanish government (PID2019-107158GB-I00 and PID2020-118145RB-I00) and Italian government (PIANO DI SOSTEGNO ALLA RICERCA 2020—Linea 2 azione B, DEFENS) are acknowledged.

Appendix A. Supplementary data

Supplementary data to this article can be found online at https://doi.org/10.1016/j.ijbiomac.2023.124794.

References

[1] S. Benabou, A. Aviñó, R. Eritja, C. González, R. Gargallo, Fundamental aspects of the nucleic acid i-motif structures, RSC Adv. 4 (2014) 26956–26980, https://doi.org/10.1039/C4RA02129K.
[2] H.A. Assi, M. Garavís, C. González, M.J. Damha, I-motif DNA: structural features and significance to cell biology, Nucleic Acids Res. 46 (2018) 8038–8056, https://doi.org/10.1093/nar/gky735.
[3] M. Cheng, D. Qiu, L. Tamon, E. Ištvánková, P. Víšková, S. Amrane, A. Guédin, J. Chen, L. Lacroix, H. Ju, L. Trantírek, A.B. Sahakyan, J. Zhou, J.-L. Mergny, Thermal and pH stabilities of i-DNA: confronting in vitro experiments with models and in-cell NMR data, Angew. Chem. Int. Ed. 60 (2021) 10286–10294, https://doi.org/10.1002/anie.202016801.
[4] E.P. Wright, J.L. Huppert, Z.A.E. Waller, Identification of multiple genomic DNA sequences which form i-motif structures at neutral pH, Nucleic Acids Res. 45 (2017) 2951–2959, https://doi.org/10.1093/nar/gkx090.
[5] M. Zeraati, D.B. Langley, P. Schofield, A.L. Moye, R. Rouet, W.E. Hughes, T. M. Bryan, M.E. Dinger, D. Christ, I-motif DNA structures are formed in the nuclei of human cells, Nat. Chem. 10 (2018) 631–637, https://doi.org/10.1038/s41557-018-0046-3.
[6] S. Dzatko, M. Krafcikova, R. Hänsel-Hertsch, T. Fessl, R. Fiala, T. Loja, D. Krafcik, J.-L. Mergny, S. Foldynova-Trantirkova, L. Trantirek, Evaluation of the stability of DNA i-motifs in the nuclei of living mammalian cells, Angew. Chem. Int. Ed. 57 (2018) 2165–2169, https://doi.org/10.1002/anie.201712284.
[7] S.L. Brown, S. Kendrick, The I-motif as a molecular target: more than a complementary DNA secondary structure, Pharmaceuticals 14 (2021) 1–25, https://doi.org/10.3390/ph14020096.
[8] R. Gargallo, A. Aviñó, R. Eritja, P. Jarosova, S. Mazzini, L. Scaglioni, P. Taborsky, Study of alkaloid berberine and its interaction with the human telomeric i-motif DNA structure, Spectrochim. Acta A Mol. Biomol. Spectrosc. 248 (2021), 119185, https://doi.org/10.1016/j.saa.2020.119185.
[9] F. Berthiol, J. Boissieras, H. Bonnet, M. Pierrot, C. Philouze, J.-F. Poisson, A. Granzhan, J. Dejeu, E. Defrancq, Novel synthesis of IMC-48 and affinity evaluation with different i-motif DNA sequences, Molecules 28 (2023) 682, https://doi.org/10.3390/molecules28020682.
[10] K.W. Lim, P. Jenjaroenpun, Z.J. Low, Z.J. Khong, Y.S. Ng, V.A. Kuznetsov, A. T. Phan, Duplex stem-loop-containing quadruplex motifs in the human genome: a combined genomic and structural study, Nucleic Acids Res. 43 (2015) 5630–5646, https://doi.org/10.1093/nar/gkv355.
[11] C.E. Kaiser, N.A. Van Ert, P. Agrawal, R. Chawla, D. Yang, L.H. Hurley, Insight into the complexity of the i-motif and G-quadruplex DNA structures formed in the KRAS promoter and subsequent drug-induced gene repression, J. Am. Chem. Soc. 139 (2017) 8522–8536, https://doi.org/10.1021/jacs.7b02046.
[12] J.L. Mergny, D. Sen, DNA quadruple helices in nanotechnology, Chem. Rev. 119 (2019) 6290–6325, https://doi.org/10.1021/acs.chemrev.8b00629.
[13] A. Dembska, The analytical and biomedical potential of cytosine-rich oligonucleotides: a review, Anal. Chim. Acta 930 (2016) 1–12, https://doi.org/10.1016/j.aca.2016.05.007.
[14] I. Serrano-Chacón, B. Mir, N. Escaja, C. González, Structure of i-Motif/Duplex junctions at neutral pH, J. Am. Chem. Soc. 143 (2021) 12919–12923, https://doi.org/10.1021/jacs.1c04679.
[15] B. Mir, I. Serrano, D. Buitrago, M. Orozco, N. Escaja, C. González, Prevalent sequences in the human genome can form mini i-motif structures at physiological pH, J. Am. Chem. Soc. 139 (2017) 13985–13988, https://doi.org/10.1021/jacs.7b07383.
[16] S. Mazzini, S. Princiotto, R. Artali, L. Musso, A. Aviñó, R. Eritja, R. Gargallo, S. Dallavalle, Exploring the interaction of G-quadruplex binders with a (3 + 1) hybrid G-quadruplex forming sequence within the PARP1 gene promoter region, Molecules 27 (2022) 4792, https://doi.org/10.3390/molecules27154792.
[17] N. Ruiz, P. Jarosova, P. Taborsky, R. Gargallo, Study of the interaction of the palmatine alkaloid with hybrid G-quadruplex/duplex and i-motif/duplex DNA structures, Biophys. Chem. 281 (2022), 106715, https://doi.org/10.1016/j.bpc.2021.106715.
[18] O.Y. Fedoroff, A. Rangan, V.V. Chemeris, L.H. Hurley, Cationic porphyrins promote the formation of i-motif DNA and bind peripherally by a nonintercalative mechanism, Biochemistry 39 (2000) 15083–15090, https://doi.org/10.1021/bi001528j.
[19] S. Fernández, R. Eritja, A. Aviñó, J. Jaumot, R. Gargallo, Influence of pH, temperature and the cationic porphyrin TMPyP4 on the stability of the i-motif formed by the 5′-(C3TA2)4–3′ sequence of the human telomere, Int. J. Biol. Macromol. 49 (2011) 729–736, https://doi.org/10.1016/j.ijbiomac.2011.07.004.
[20] W.A. Kibbe, OligoCalc: an online oligonucleotide properties calculator, Nucleic Acids Res. 35 (2007) 43–46, https://doi.org/10.1093/nar/gkm234.
[21] R. Cincinelli, L. Musso, L. Merlini, G. Giannini, L. Vesci, F.M. Milazzo, N. Carenini, P. Perego, S. Penco, R. Artali, F. Zunino, C. Pisano, S. Dallavalle, 7-Azaindole-1-carboxamides as a new class of PARP-1 inhibitors, Bioorg. Med. Chem. 22 (2014) 1089–1103, https://doi.org/10.1016/j.bmc.2013.12.031.
[22] L. Musso, S. Mazzini, A. Rossini, L. Castagnoli, L. Scaglioni, R. Artali, M. di Nicola, F. Zunino, S. Dallavalle, C-MYC G-quadruplex binding by the RNA polymerase I inhibitor BMH-21 and analogues revealed by a combined NMR and biochemical approach, Biochim. Biophys. Acta Gen. Subj. 1862 (2018) 615–629, https://doi.org/10.1016/j.bbagen.2017.12.002.
[23] K.J. Breslauer, Extracting thermodynamic data from equilibrium melting curves for oligonucleotide order-disorder transitions, Methods Enzymol. 259 (1995) 221–242, https://doi.org/10.1016/0076-6879(95)59046-3.
[24] J.-L. Mergny, L. Lacroix, UV melting of G-quadruplexes, Curr. Protoc. Nucleic Acid Chem. 37 (2009), https://doi.org/10.1002/0471142700.nc1701s37, 17.1.1-17.1.15.
[25] R.D. Gray, J.B. Chaires, Analysis of multidimensional Q-quadruplex melting curves, curr protoc nucleic acid chem, Unit 17 (4) (2011), https://doi.org/10.1002/0471142700.nc1704s45.
[26] R. Gargallo, Hard/Soft hybrid modeling of temperature-induced unfolding processes involving G-quadruplex and i-motif nucleic acid structures, Anal. Biochem. 466 (2014) 4–15, https://doi.org/10.1016/j.ab.2014.08.008.

[27] R.M. Dyson, S. Kaderli, G.A. Lawrance, M. Maeder, A.D. Zunderbuhler, Second order global analysis: the evaluation of series of spectrophotometric titrations for improved determination of equilibrium constants, Anal. Chim. Acta 353 (1997) 381–393, https://doi.org/10.1016/S0003-2670(97)87800-2.
[28] S. Benabou, R. Ferreira, A. Aviñó, C. González, S. Lyonnais, M. Solà, R. Eritja, J. Jaumot, R. Gargallo, Solution equilibria of cytosine- and guanine-rich sequences near the promoter region of the n-myc gene that contain stable hairpins within lateral loops, Biochim. Biophys. Acta Gen. Subj. 1840 (2014) 41–52, https://doi.org/10.1016/j.bbagen.2013.08.028.
[29] S. Benabou, A. Aviñó, S. Lyonnais, C. González, R. Eritja, A. de Juan, R. Gargallo, I-motif structures in long cytosine-rich sequences found upstream of the promoter region of the SMARCA4 gene, Biochimie 140 (2017), https://doi.org/10.1016/j.biochi.2017.06.005.
[30] A. Navarro, S. Benabou, R. Eritja, R. Gargallo, Influence of pH and a porphyrin ligand on the stability of a G-quadruplex structure within a duplex segment near the promoter region of the SMARCA4 gene, Int. J. Biol. Macromol. 159 (2020) 383–393, https://doi.org/10.1016/j.ijbiomac.2020.05.062.
[31] J.N. Zadeh, C.D. Steenberg, J.S. Bois, B.R. Wolfe, M.B. Pierce, A.R. Khan, R. M. Dirks, N.A. Pierce, NUPACK: analysis and design of nucleic acid systems, J. Comput. Chem. 32 (2011) 170–173, https://doi.org/10.1002/JCC.21596.
[32] A. Bedrat, L. Lacroix, J.-L. Mergny, Re-evaluation of G-quadruplex propensity with G4Hunter, Nucleic Acids Res. 44 (2016) 1746–1759, https://doi.org/10.1093/nar/gkw006.
[33] J. Kypr, I. Kejnovska, D. Renciuk, M. Vorlickova, Circular dichroism and conformational polymorphism of DNA, Nucleic Acids Res. 37 (2009) 1713–1725, https://doi.org/10.1093/nar/gkp026.
[34] S. Benabou, S. Mazzini, A. Aviñó, R. Eritja, R. Gargallo, A pH-dependent bolt involving cytosine bases located in the lateral loops of antiparallel G-quadruplex structures within the SMARCA4 gene promotor, Sci. Rep. 9 (2019) 15807, https://doi.org/10.1038/s41598-019-52311-5.
[35] H.A. Day, P. Pavlou, Z.A.E. Waller, I-motif DNA: structure, stability and targeting with ligands, Bioorg. Med. Chem. 22 (2014) 4407–4418, https://doi.org/10.1016/j.bmc.2014.05.047.
[36] S.S. Masoud, K. Nagasawa, I-motif-binding ligands and their effects on the structure and biological functions of i-motif, Chem. Pharm. Bull. 66 (2018) 1091–1103.
[37] A. Pagano, N. Iaccarino, M.A.S. Abdelhamid, D. Brancaccio, E.U. Garzarella, A. di Porzio, E. Novellino, Z.A.E. Waller, B. Pagano, J. Amato, A. Randazzo, Common G-quadruplex binding agents found to interact with i-motif-forming DNA: unexpected multi-target-directed compounds, Front. Chem. 6 (2018). https://www.frontiersin.org/articles/10.3389/fchem.2018.00281.
[38] G. Cosa, K.-S. Focsaneanu, J.R.N. McLean, J.P. McNamee, J.C. Scaiano, Photophysical properties of fluorescent DNA-dyes bound to single- and double-stranded DNA in aqueous buffered solution, Photochem. Photobiol. 73 (2007) 585–599, https://doi.org/10.1562/0031-8655(2001)0730585PPOFDD2.0.CO2.
[39] E. Ruggiero, S. Lago, P. Šket, M. Nadai, I. Frasson, J. Plavec, S.N. Richter, A dynamic i-motif with a duplex stem-loop in the long terminal repeat promoter of the HIV-1 proviral genome modulates viral transcription, Nucleic Acids Res. 47 (2019) 11057–11068, https://doi.org/10.1093/nar/gkz937.
[40] L. Shi, P. Peng, J. Zheng, Q. Wang, Z. Tian, H. Wang, T. Li, I-Motif/miniduplex hybrid structures bind benzothiazole dyes with unprecedented efficiencies: a generic light-up system for label-free DNA nanoassemblies and bioimaging, Nucleic Acids Res. 48 (2020) 1681–1690, https://doi.org/10.1093/nar/gkaa020.
[41] J. Amato, N. Iaccarino, F. D'Aria, F. D'Amico, A. Randazzo, C. Giancola, A. Cesàro, S. Di Fonzo, B. Pagano, Conformational plasticity of DNA secondary structures: probing the conversion between i-motif and hairpin species by circular dichroism and ultraviolet resonance raman spectroscopies, Phys. Chem. Chem. Phys. 24 (2022) 7028–7044, https://doi.org/10.1039/d2cp00058j.
[42] S. Benabou, M. Garavís, S. Lyonnais, R. Eritja, C. González, R. Gargallo, Understanding the effect of the nature of the nucleobase in the loops on the stability of the i-motif structure, Phys. Chem. Chem. Phys. 18 (2016) 7997–8004, https://doi.org/10.1039/C5CP07428B.
[43] M. Mondal, Y.Q. Gao, Microscopic insight into pH-dependent conformational dynamics and Noncanonical Base pairing in telomeric i-motif DNA, J. Phys. Chem. Lett. (2022) 5109–5115, https://doi.org/10.1021/acs.jpclett.2c00640.
[44] I. Serrano-Chacón, B. Mir, L. Cupellini, F. Colizzi, M. Orozco, N. Escaja, C. González, pH-dependent capping interactions induce large-scale structural transitions in i-motifs, J. Am. Chem. Soc. (2023), https://doi.org/10.1021/jacs.2c13043.
[45] H. Bonnet, M. Morel, A. Devaux, J. Boissieras, A. Granzhan, B. Elias, T. Lavergne, J. Dejeu, E. Defrancq, Assessment of presumed small-molecule ligands of telomeric i-DNA by biolayer interferometry (BLI), Chem. Commun. 58 (2022) 5116–5119, https://doi.org/10.1039/D2CC00836J.
[46] O.Yu. Fedoroff, A. Rangan, V.V. Chemeris, L.H. Hurley, Cationic porphyrins promote the formation of i-motif DNA and bind peripherally by a nonintercalative mechanism, Biochemistry 39 (2000) 15083–15090, https://doi.org/10.1021/bi001528j.
[47] Y. Yang, H. Fu, C. Qian, H. Li, D.D.Y. Chen, Characterization of interaction between Bcl-2 oncogene promoter I-motif DNA and flavonoids using electrospray ionization mass spectrometry and pressure-assisted capillary electrophoresis frontal analysis, Talanta 215 (2020), 120885, https://doi.org/10.1016/j.talanta.2020.120885.
[48] S. Takahashi, S. Bhattacharjee, S. Ghosh, N. Sugimoto, S. Bhowmik, Preferential targeting cancer-related i-motif DNAs by the plant flavonol fisetin for theranostics applications, Sci. Rep. 10 (2020) 2504, https://doi.org/10.1038/s41598-020-59343-2.
[49] K.L. Irving, J.J. King, Z.A.E. Waller, C.W. Evans, N.M. Smith, Stability and context of intercalated motifs (i-motifs) for biological applications, Biochimie 198 (2022) 33–47, https://doi.org/10.1016/j.biochi.2022.03.001.
[50] H. Alniss, B. Zamiri, M. Khalaj, C.E. Pearson, R.B. Macgregor Jr., Thermodynamic and spectroscopic investigations of TMPyP4 association with guanine- and cytosine-rich DNA and RNA repeats of C9orf72, Biochem. Biophys. Res. Commun. 495 (2018) 2410–2417, https://doi.org/10.1016/j.bbrc.2017.12.108.